

JOINT ESTIMATION OF ACTIVITY DISTRIBUTION AND ATTENUATION MAP FOR TOF-PET USING ALTERNATING DIRECTION METHOD OF MULTIPLIER

Se Young Chun^{*}, Kyeong Yun Kim[†], Jae Sung Lee[†], Jeffrey A Fessler[‡]

^{*} Ulsan National Institute of Science and Technology (UNIST)

[†] Seoul National University, [‡] University of Michigan - Ann Arbor

ABSTRACT

Recent advances in TOF PET joint estimation of activity and attenuation showed that activity and attenuation can be determined up to a global constant scale without severe cross-talk. MLAA was first proposed to estimate activity and attenuation map simultaneously, and then MLACF was developed to estimate activity and attenuation compensation factor (ACF). MLAA incorporated prior knowledge on the zero attenuation value outside body area to determine global scalar, but was slow to converge. MLACF converged much faster than MLAA, but required knowing total activity level in advance. We propose a new optimization method based on variable splitting and alternating direction method of multiplier (MLADMM). Our proposed MLADMM achieved fast convergence rate comparable to MLACF without knowing total activity level. MLADMM also has a potential to use more sophisticated MR-based prior for attenuation in PET-MR.

Index Terms— TOF PET, Joint estimation, ADMM

1. INTRODUCTION

Attenuation correction is important for accurate quantitation in emission tomography. Sequentially acquired CT along with emission data has been dominantly used in clinics for attenuation correction. However, this procedure has a few disadvantages: possible misalignment between emission image and CT and additional radiation dose due to CT.

Simultaneous estimation of activity and attenuation from emission data only can be a potential solution for these problems, but had very limited success due to severe cross-talk between activity and attenuation. Recently, Defrise *et al.* showed that one can determine activity and attenuation from TOF-PET data up to a global constant scale [1]. Based on this finding, two algorithms were proposed: maximum likelihood activity and attenuation reconstruction (MLAA) [2] and maximum likelihood activity and ACF (MLACF) [3]. MLACF

showed faster convergence rate in terms of likelihood (however, [3] reported that MLACF had slower convergence in terms of mean squared difference) and required lower computation complexity than MLAA.

However, MLACF also has a few disadvantages: MLACF depends on rather unrealistic assumption of known total activity level and cannot use image-domain priors for estimating attenuation such as a MR-based prior in TOF PET-MR [4]. To determine a constant scaling, both methods used prior knowledge: zero attenuation outside body contour (MLAA) and known total activity level (MLACF). Slight mis-segmentation for body contour could be compensated by using a regularizer that encourages attenuation map to have either zero or tissue attenuation. In contrast, measuring total activity level before reconstruction is challenging, so it is somewhat impractical [3].

This paper proposes a new optimization method using alternating direction method of multiplier (ADMM). In this method, activity, attenuation map, and ACF will be estimated jointly and constant scaling will be determined by using a prior on zero attenuation outside body contour. Our proposed method does not require known total activity level and can accommodate any prior for the attenuation map such as MR-based prior in PET-MR. Each sub-problem is solved by using an optimization transfer method based on De Pierro's lemma [5]. We also show that the MLACF algorithm can be derived based on the well-established optimization transfer method.

Section 2 derives a new algorithm for TOF PET joint estimation of activity and attenuation using variable splitting and ADMM. Section 3 presents 2D TOF PET simulation results using XCAT phantom for noiseless data and noisy data.

2. METHOD

2.1. Previous Methods

The expected count \bar{y}_{it} for the line of response (LOR) i and time difference t in TOF-PET can be expressed:

$$\bar{y}_{it}(\lambda, \mu) = \exp \left\{ - \sum_k l_{ik} \mu_k \right\} \sum_{j=1}^J c_{ijt} \lambda_j + s_{it} \quad (1)$$

This research was supported in part by Basic Science Research Program through the National Research Foundation of Korea (NRF) funded by the Ministry of Science, ICT & Future Planning (NRF-2014R1A1A1007928), Republic of Korea, in part by NRF-2014M3C7034000, Republic of Korea, and in part by NIH U01 EB018753, USA. (*email: sychun@unist.ac.kr)

where λ_j, μ_k are the activity and attenuation coefficient at voxel j and k , respectively. J is the total number of voxels, c_{ijt} is the sensitivity of the detector at (i, t) for activity in voxel j in absence of attenuation, l_{ik} is the intersection length of LOR i with voxel k , and s_{it} is the expected contribution of scatter and/or randoms.

Then, for the measured data y_{it} , which is a Poisson realization with the mean \bar{y}_{it} , the log-likelihood function is

$$\mathcal{L}(\lambda, \mu; y) = \sum_{it} y_{it} \log \bar{y}_{it}(\lambda, \mu) - \bar{y}_{it}(\lambda, \mu). \quad (2)$$

MLAA obtains the maximum likelihood (ML) estimate

$$(\hat{\lambda}, \hat{\mu}) = \arg \max_{\lambda \geq 0, \mu \geq 0} \mathcal{L}(\lambda, \mu; y) - \eta R(\mu) \quad (3)$$

where $R(\cdot)$ is a regularizer that encourages μ to be either zero or tissue attenuation outside the body area only. MLAA alternatively maximizes (2) with respect to λ and μ .

Instead of estimating attenuation map μ , which is usually a nuisance parameter, ACF can be estimated. Then, (1) can be modified as follows [3]:

$$\bar{y}_{it}(\lambda, a) = a_i \sum_{j=1}^J c_{ijt} \lambda_j + s_{it} = p_{it} a_i + s_{it}. \quad (4)$$

Thus, MLACF performs the following maximization to estimate activity and ACF:

$$(\hat{\lambda}, \hat{a}) = \arg \max_{\lambda \geq 0, a \geq 0} \mathcal{L}(\lambda, a; y) \quad (5)$$

where

$$\mathcal{L}(\lambda, a; y) = \sum_{it} y_{it} \log \bar{y}_{it}(\lambda, a_i) - \bar{y}_{it}(\lambda, a_i). \quad (6)$$

To determine a global constant scaling, for each iteration, total activity level compensation was done in [3] without changing the value of likelihood ($\lambda = \delta \lambda, a = a/\delta$ such that $\delta \lambda$ contains known total activity level. A scalar constant δ should be obtained at each iteration). Note that image domain prior can not be used in MLACF.

2.2. Proposed Method

We re-formulate the original problem of MLAA in (3) using a single variable splitting, which is also used in [6], as follows:

$$(\hat{\lambda}, \hat{\mu}) = \arg \min_{\lambda \geq 0, \mu \geq 0, 0 \leq a \leq 1} -\mathcal{L}(\lambda, a; y) + \eta R(\mu) \quad (7)$$

subject to $a_i = \exp\{-\sum_k l_{ik} \mu_k\}$. To solve this constrained optimization problem, we construct an augmented Lagrangian term $\text{AL}(\lambda, \mu, a, d)$

$$-\mathcal{L}(\lambda, a; y) + \eta R(\mu) + \frac{\alpha}{2} \sum_i (a_i - e^{-\sum_k l_{ik} \mu_k} - d_i)^2 \quad (8)$$

where d is a Lagrangian multiplier vector that is scaled by α and $\alpha > 0$ is a design parameter that may affect the speed of convergence and which local minimizer is found. We optimize $\text{AL}(\cdot)$ using the following algorithm:

For $n = 0, 1, 2, \dots$

$$\hat{a}^{(n+1)} \in \arg \min_{0 \leq a \leq 1} \text{AL}(\hat{\lambda}^{(n)}, \hat{\mu}^{(n)}, a, \hat{d}^{(n)}) \quad (9)$$

$$\hat{\lambda}^{(n+1)} \in \arg \min_{\lambda \geq 0} -\mathcal{L}(\lambda, \hat{a}^{(n+1)}; y) \quad (10)$$

$$\hat{\mu}^{(n+1)} \in \arg \min_{\mu \geq 0} \frac{1}{2} \|\hat{a}^{(n+1)} - e^{-\mathbf{L}\mu} - \hat{d}^{(n)}\|^2 + \eta R(\mu) \quad (11)$$

$$d^{(n+1)} = d^{(n)} - (\hat{a}^{(n+1)} - e^{-\mathbf{L}\hat{\mu}^{(n+1)}}) \quad (12)$$

End

where \mathbf{L} is a matrix with elements l_{ij} and $e^{(\cdot)}$ is a component-wise function. For each sub-problem, more than one iteration is possible. The sub-problem (10) can be solved using standard OSEM algorithm for fixed \hat{a} , which is also used in MLACF [3]. The sub-problem (12) is solved using one step gradient ascent. The following sections derive algorithms for the sub-problems (9) and (11) using optimization transfer. Optimization for each sub-problem can be accelerated using ordered subset (OS) approximation [7]. Although (8) does not have local minima for (λ, a) (other than the global minimum) for consistent TOF measurements [3], it is not convex for μ . Thus, $\text{AL}(\lambda, \mu, a, d)$ may have many local minima with respect to (λ, μ) . More investigation is needed for avoiding local minima.

2.3. Algorithm for Sub-Problem (9)

For the sub-problem (9), we used De Pierro's lemma to derive a surrogate function for the likelihood of the original problem [5]:

$$\sum_{it} h_{it}(p_{it} a_i + s_{it}) \leq \sum_{it} p_{it} \frac{a_i^n}{\bar{y}_{it}^n} h_{it} \left(\frac{a_i}{a_i^n} \bar{y}_{it}^n \right) + \frac{s_{it}}{\bar{y}_{it}^n} h_{it}(\bar{y}_{it}^n)$$

where $\bar{y}_{it}^n = \sum_{\xi} \hat{a}_i^n c_{i\xi t} \lambda_{\xi} + s_{it}$ and $h_{it}(z) = z - y_{it} \log z$. By removing constant terms, a separable quadratic surrogate function of (8) for parameter a_i becomes

$$Q_i(a_i; \hat{a}_i^n) = p_i a_i - \hat{a}_i^n e(\hat{a}_i^n) \log a_i + \frac{\alpha}{2} (a_i - b_i^n)^2 \quad (13)$$

where $p_i = \sum_t p_{it}$, $e(a_i^n) = \sum_t p_{it} y_{it} / \bar{y}_{it}^n$, and $b_i^n = \exp(-[\mathbf{L}\hat{\mu}^n]_i) + \hat{d}_i^n$. Then, the minimizer of (13) with respect to a_i is found by zeroing its derivative and using the quadratic formula. This optimization transfer based algorithm is guaranteed to converge monotonically. Note that if $\alpha = 0$, then the minimizer of (13) is reduced to the same algorithm for the sub-iteration of MLACF [3]. Regularizers can be incorporated in this algorithm as shown in [5].

2.4. Algorithm for Sub-Problem (11)

For the subproblem (11) with non-convex cost function, we used a nested optimization transfer that was applied to transmission tomography reconstruction [8]. Firstly, a nonseparable quadratic surrogate q_i for (11) is

$$\sum_i g_i([\mathbf{L}\mu]_i) \leq \sum_i q_i([\mathbf{L}\mu]_i; l_i^n) \quad (14)$$

where $l_i^n = [\mathbf{L}\mu^n]_i$, $g_i(l) = (e^{-l} - a_i + d_i)^2 / 2$,

$$q_i(l; l_i^n) = g_i(l_i^n) + \dot{g}_i(l_i^n)(l - l_i^n) + \frac{1}{2}c_i(l_i^n)(l - l_i^n)^2$$

where the optimum curvature c_i is described in [8]. Then, a separable quadratic surrogate (SQS) for (14) can be derived using De Pierro's lemma [5]:

$$\sum_i q_i([\mathbf{L}\mu]_i; l_i^n) \leq \sum_{ij} \frac{l_{ij}}{\gamma_i} q_i(\gamma_i(\mu_j - \mu_j^n) + [\mathbf{L}\mu^n]_i; l_i^n) \quad (15)$$

where $\gamma_i = \sum_j l_{ij}$. This SQS with a separable surrogate regularizer $\sum_j r_j(\mu_j)$ for $R(\mu)$ can be minimized using 1D Newton-Raphson type sub-iterations:

$$\mu_j^{n+1} = \mu_j^n - \frac{1}{d_j + \eta \ddot{r}_j(\mu_j)} \left\{ \sum_i \frac{\partial g_i([\mathbf{L}\mu^n]_i)}{\partial \mu_j} + \eta \dot{r}_j(\mu_j) \right\}$$

where $d_j = \sum_i l_{ij} \gamma_i c_i(l_i^n)$ and $\dot{r}_j(\cdot), \ddot{r}_j(\cdot)$ are the first and second order derivatives of $r_j(\cdot)$, respectively. One can find a separable surrogate regularizer for any $R(\mu)$ using De Pierro's lemma (see [8] for examples). In this work, we chose to use the same regularizer as that in MLAA [2], which is already separable.

3. SIMULATION RESULTS

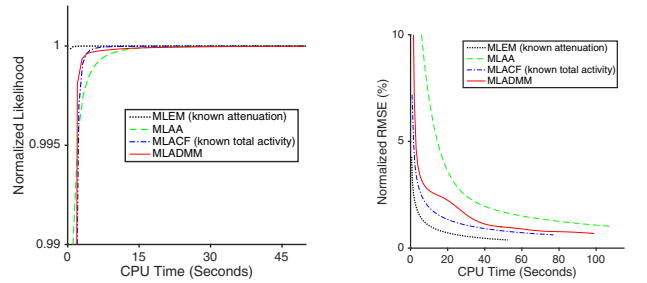
3.1. Setup

TOF PET simulation was performed with a 2D XCAT phantom [9]. The 2D system matrix modeled Discovery GE 690 TOF PET with the image size 180 x 180 pixels (3.27 x 3.27 mm), TOF sinogram of 281 radial bins, 288 angular bins and 11 TOF bins (the simulated TOF resolution was 500 ps). 50% random was added and it is assumed to be known during the reconstruction. Both noiseless and noisy sinograms were used for testing the proposed method.

In the reconstruction, 100 iterations with 32 subsets were used. We performed MLEM (assuming known CT as a baseline for comparison), MLAA, MLACF, and the proposed method (MLADMM). The ratios of sub-iterations for attenuation update to sub-iteration for activity update were 5:1 (MLAA), 3:1 (MLACF), 3:2:1 (MLADMM, attenuation map: ACF: activity). Note that MLAA and MLADMM used a regularizer that encourages zero or tissue attenuation value outside the body area and MLACF assumed known total activity level before reconstruction.

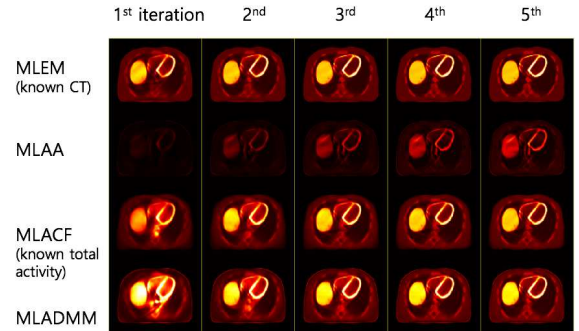
3.2. Result: Noiseless Sinogram

Fig. 1 shows the results for noiseless TOF sinogram data. Normalized likelihood in (a) shows that the initial convergence rate of the proposed MLADMM is comparable to that of MLACF and much faster than that of MLAA. Note that MLACF requires known total activity to achieve fast convergence. Normalized root mean squared error (RMSE) between estimated and true activity images in (b) also shows that MLADMM converged faster than MLAA, which is comparable to MLACF. First five estimated images (with 32 subsets) of activity (c) and ACF (d) show that MLADMM yielded activity comparable to MLACF and better ACF than MLAA and MLACF.

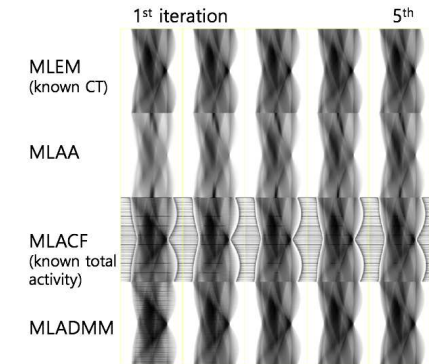


(a) Normalized likelihood

(b) Normalized RMSE



(c) First five iterations of activity image



(d) First five iterations of ACF (log scale)

Fig. 1. Results from noiseless TOF sinogram.

3.3. Result: Noisy Sinogram

Fig. 2 shows the results for moderately noisy TOF sinogram data. These results show similar tendency to those in noiseless sinogram results. Fig. 2 (a) shows that MLADMM yielded fast initial convergence rate over MLAA and (b) shows that MLADMM achieved comparable minimum RMSE to MLACF without knowing total activity. Note that all methods in (b) yielded higher RMSE for more iteration since the original problem is not regularized. One can use either a regularizer for activity or early stop rule. First five iterations of activity (c) and attenuation (d) also show that MLADMM yielded comparable activity image to MLEM and MLACF without knowing either CT or total activity level and achieved similar quality of attenuation over MLAA and MLACF.

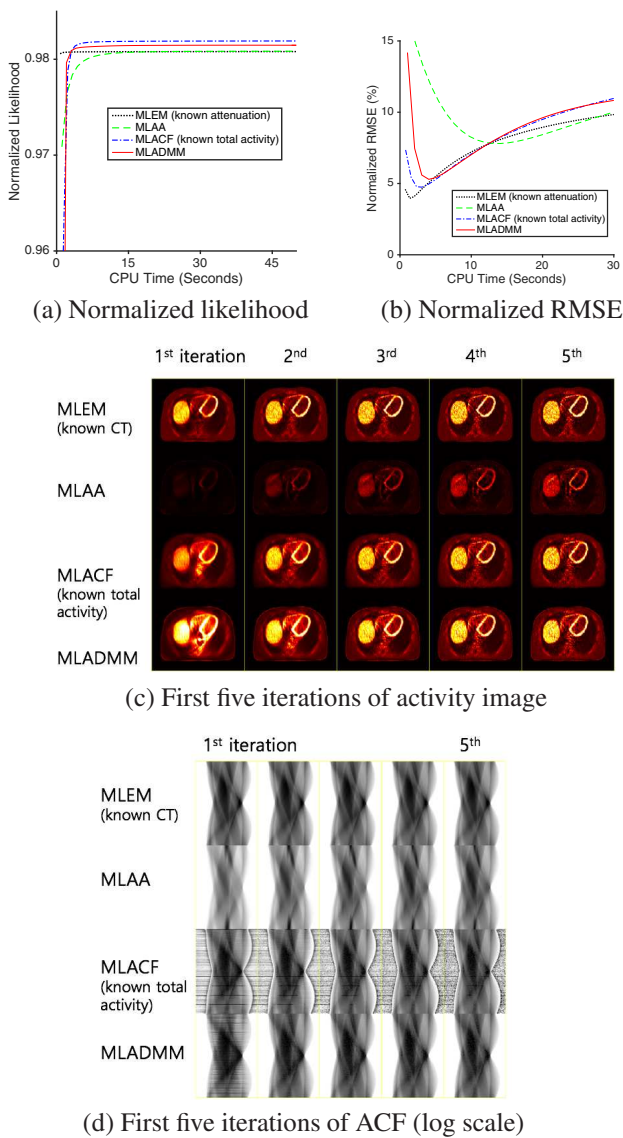


Fig. 2. Results from moderately noisy TOF sinogram.

4. CONCLUSION

We proposed a new method for joint estimation of activity and attenuation from TOF sinogram data. MLADMM converged faster than MLAA and also achieved comparable results to MLACF without knowing total activity level. MLADMM has potential to incorporate image-domain prior in PET-MR.

5. REFERENCES

- [1] Michel Defrise, Ahmadreza Rezaei, and Johan Nuyts, "Time-of-flight PET data determine the attenuation sinogram up to a constant," *Physics in Medicine and Biology*, vol. 57, no. 4, pp. 885–899, Feb. 2012.
- [2] Ahmadreza Rezaei, Michel Defrise, Girish Bal, Christian Michel, Maurizio Conti, Charles Watson, and Johan Nuyts, "Simultaneous reconstruction of activity and attenuation in time-of-flight PET," *IEEE Transactions on Medical Imaging*, vol. 31, no. 12, pp. 2224–2233, Dec. 2012.
- [3] Ahmadreza Rezaei, Michel Defrise, and Johan Nuyts, "ML-reconstruction for TOF-PET with simultaneous estimation of the attenuation factors," *IEEE Transactions on Medical Imaging*, vol. 33, no. 7, pp. 1563–1572, July 2014.
- [4] Abolfazl Mehranian and Habib Zaidi, "Joint Estimation of Activity and Attenuation in Whole-Body TOF PET/MRI Using Constrained Gaussian Mixture Models," *IEEE Transactions on Medical Imaging*, vol. 34, no. 9, pp. 1808–1821, Sept. 2015.
- [5] A R De Pierro, "A modified expectation maximization algorithm for penalized likelihood estimation in emission tomography," *IEEE Transactions on Medical Imaging*, vol. 14, no. 1, pp. 132–137, 1995.
- [6] Se Young Chun, Yuni K Dewaraja, and Jeffrey A Fessler, "Alternating direction method of multiplier for tomography with nonlocal regularizers," *IEEE Transactions on Medical Imaging*, vol. 33, no. 10, pp. 1960–1968, Oct. 2014.
- [7] H M Hudson and R S Larkin, "Accelerated image reconstruction using ordered subsets of projection data," *IEEE Transactions on Medical Imaging*, vol. 13, no. 4, pp. 601–609, 1994.
- [8] H Erdoğ an and J A Fessler, "Ordered subsets algorithms for transmission tomography," *Physics in Medicine and Biology*, vol. 44, no. 11, pp. 2835–2851, Nov. 1999.
- [9] W P Segars, G Sturgeon, S Mendonca, Jason Grimes, and B M W Tsui, "4D XCAT phantom for multimodality imaging research," *Medical Physics*, vol. 37, no. 9, pp. 4902–15, 2010.